Asian Journal of Chemistry; *Vol. 24, No. 6 (2012), 2546-2550*

ASIAN JOURNAL OF CHEMISTRY

www.asianjournalofchemistry.co.in

Fabrication and Characterization of Single-Walled Carbon Nanotubes from La_2O_3 Nanoparticles by Ethanol Chemical Vapour Deposition

CHUNYAN WANG*, JUN SHI and ZHANGGAO LE*

Department of Applied Chemistry, East China Institute of Technology, Fuzhou 344000, P.R. China

*Corresponding authors: Tel/Fax: +86 794 8258320; E-mail: chunyanwang@ecit.cn; zhgle@ecit.cn

(*Received*: 11 May 2011; *Accepted*: 13 January 2012) AJC-10941

The lanthanum sesquioxide is an active and efficient catalyst for the growth of single-walled carbon nanotubes by a catalytic chemical vapour deposition process. Horizontally superlong well-oriented single-walled carbon nanotubes on SiO_2/Si wafer surface can be fabricated *via* EtOH as carbon source when the temperature is in the range of 700-950 ºC. The carbon nanostructures are characterized by electronic microscopy, atomic force microscopy, Raman spectroscopy, X-ray diffraction, *etc*. As-grown single-walled carbon nanotubes from La_2O_3 have compatibly high quality and purity. This novel oxide provides a new experimental avenue to understand the growth mechanism of single-walled carbon nanotubes and a series of replaceable catalysts for nanotubes growth has been developed, which may be helpful for their controllable synthesis.

Key Words: Nano materials, Vapour deposition, Defects.

INTRODUCTION

After the discovery of carbon nanotubes (CNTs)[1,2], much attention has been paid to their outstanding mechanical and electronic properties due to their unique structure. Especially, single-walled carbon nanotubes (SWNTs) can behave as metal or semiconductor depending on the tube diameter and chirality. Furthermore, their properties contain a potential for various applications, such as quantum wire, gas storage, field effect transistor, field emission devices and nanoreactor[3-6]. Therefore, it is important to control the diameter and chirality of CNTs. It is well-known that the Fe family elements and their alloys are effective group of catalysts. Experimental[7] and theoretical[8,9] studies all show their high catalytic activities. However, in the past five years many other metals such as Ag, Pd, Au, Cu, Rh, Pb, Dy[10-16], semiconductors such as Si and Ge[12], carbides such as SiC[12], Fe_3C[17] and more recently Mg, Mn, Cr, Sn and Al[18,19] or oxide nanoparticles such as SiO_2, Al_2O_3, TiO_2, ZrO_2 *etc*.[20-21] have been reported to be active for SWNTs growth. Growing SWNTs on substrate has been paid a lot of attentions in recent years because it is strongly desirable for nanodevice fabrication. Therefore, these findings challenge the traditional thinking about the growth of CNTs and the role of the catalysts. Furthermore, different types of catalysts will provide more chance to understand the relationship between the catalyst and the structures of the SWNTs and thus the approach for selective growth of semiconducting single-walled carbon nanotubes (s-SWNTs) or metallic single-walled carbon nanotubes (m-SWNTs) may be found out.

To the best of our knowledge, little experiment has been studied about the superlong well-oriented SWNT arrays EtOH-chemical vapour deposition from rare earth metal oxide La_2O_3. Present results show that the SWNTs synthesized in this study have good structure with fewer defects. The successful growth of SWNTs by this new metallic oxide provides some new information to understand the growth mechanism of SWNTs and will be helpful for their controllable synthesis.

EXPERIMENTAL

Si wafer with 1 μm layer of SiO_2 was firstly cleaned by H_2SO_4/H_2O_2 solution and washed with deionized water and acetone under sonication before use. $La(NO_3)_3$ was purchased from Aldrich with purity higher than 99.99 %. The catalyst precursors were loaded onto the edges of the substrate by dipping the wafer into 1 mM ethanol solution of $La(NO_3)_3$. Then the wafer was placed into the 1 inch diameter quartz tube reactor. After the furnace was heated to 900 ºC in H_2 and lasted for 5 min, then the growth temperature was varied over a range of 700-950 ºC at 50 ºC increments, ethanol vapour was delivered by bubbling H_2 (200 sccm) into ethanol containing 1-3 % deionized water at 25-30 ºC for 10 min.

SEM images were taken from FEI NanoSEM at 1 kV, spot 4. HRTEM (Philips CM200) was operated at 200 kV. AFM images were recorded at NanoScope IIIa from Veeco, Inc. in tapping mode. Raman spectra of SWNTs on either silicon wafers were collected from JY-T64000 Raman spectroscopy by using a excitation laser lines of 632.8 nm (1.96 eV) from an air-cooled Ar^+ laser. The catalyst powder was analyzed by XRD (Bruker, D8, Cu $K_\alpha 1$, λ = 1.5406 Å).

RESULTS AND DISCUSSION

Ethanolic solution of $La(NO_3)_3$ as starting materials for the growth of carbon nanotubes (CNTs) by catalytic chemical vapour deposition (CCVD) method was carried out at different growth temperatures. The typical SEM image of the as-grown SWNT arrays at 900 ºC was shown in Fig. 1a. The inset was the high magnification SEM image (Fig. 1a$_1$) and HRTEM image (Fig. 1a$_2$), respectively. It could be seen from Fig. 1a$_1$ that the horizontally aligned SWNT arrays were uniform over a large area and the density of these parallel SWNTs is about 3-4 SWNTs/20 µm. Moreover, Fig. 1a$_2$ showed that the nanotubes grown on Si_3N_4 window was single wall. The length of the wafer was about 1.5 cm. Most of the nanotubes could grow from one side to another on the wafer, suggesting the length of the SWNT arrays in centimeter scale. During the past few years it was demonstrated that CNTs with lengths up to centimeters could be grown and they exhibited alignment with the gas flow direction[22,23]. Though this density was lower than those of aligned SWNT arrays grown on quartz[22] and sapphire[24], it was still very high reports of horizontally well-oriented SWNTs on silicon wafers[22,23]. Such large-area uniform SWNT arrays showed attractive applications in various SWNT-based nano-devices.

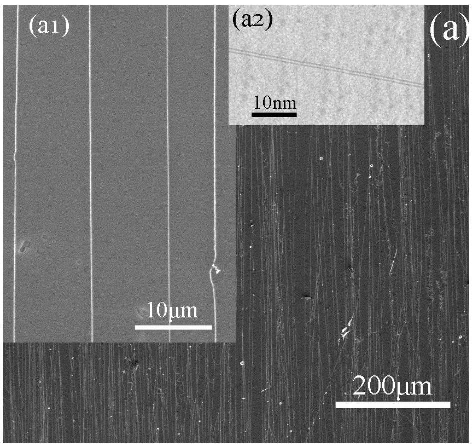

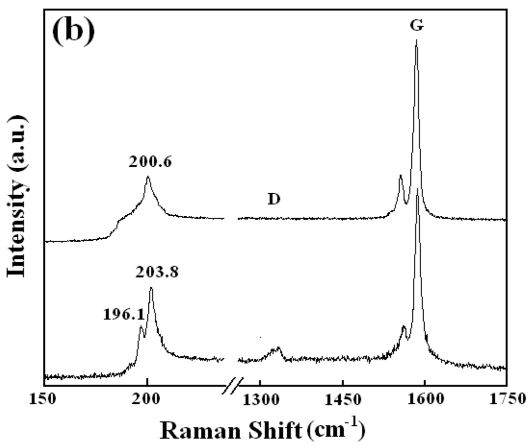

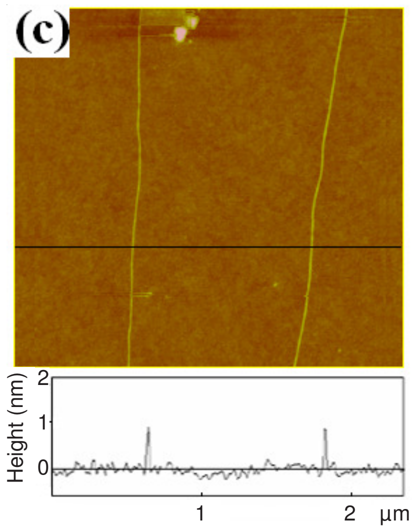

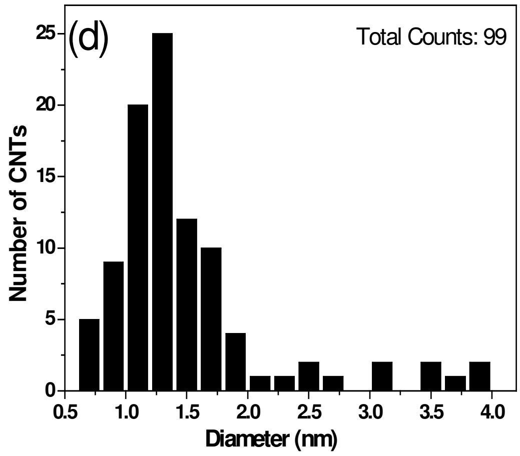

Fig. 1. (a, a$_1$) SEM image and its part magnified image of aligned SWNT arrays respectively. (a$_2$) TEM image of individual nanotube. (b) Raman spectra for the two different position of as-grown SWNTs on SiO_2/Si wafer. (c) AFM image of selected SWNTs in these arrays. (d) Distribution of diameters of SWNTs in the arrays measured by TEM. The average diameter is 1.356 nm for SWNTs

Raman spectroscopy had been proven to be a powerful tool for characterizing and revealing the detailed structure and the electronic and phonon properties of SWNTs, it could be applied to characterize the carbon nanotubes in which the radial breathing model (RBM) could be used to identify the structure and the diameter (d) of the SWNT. The two different position of the SWNT arrays on SiO_2/Si wafer Raman lasers were taken from the same excitation frequencies. Both of the typical Raman spectra were shown in Fig. 1b. It could be seen that a strong G band peak at about 1595 cm^{-1} corresponded to graphitic structure and a weak D band peak indicated a good quality of SWNTs. Furthermore, three radial breathing model peaks at around 200, 203, 196 cm^{-1} were observed. The diameters of the SWNTs were calculated to be about 1.24, 1.22, 1.27 nm according to the equation of $d = 248\ cm^{-1}/\omega$[25,26], which was within the range obtained from our AFM and TEM observations.

Fig. 1c showed the AFM image of two SWNTs in Fig. 1a. On the basis of TEM measurements on 99 tubes, we obtained the diameter distribution of the SWNTs as shown in Fig. 1d. A Gaussian fit was done and gave the most probable diameter of 1.356 nm. Most of them had a diameter of less than 2.0 nm (87 tubes in 99, *i.e*., 87.9 %). The diameters larger than 2.0 nm shown in part (d) were possibly related to small SWNT bundles or multi-walled carbon nanotubes.

To confirm that it was La_2O_3 nanoparticles acting as the catalyst during the chemical vapour deposition process, we took the energy disperse X-ray spectrum (EDX) measurement on the Cu foil after the growth of nanotubes. The results indicated the catalyst particle contain large amount of oxygen atoms as shown in Fig. 2a, suggesting that it exhibited an oxide state. In addition, it was needed to point out that Fe family and any other metal elements were not found in the sample, indicating that it was lanthanum oxide acting as catalyst in the growth process. Before the XRD was performed, we put the solid state of $La(NO_3)_3$ into porcelain boat, then it was heated at 900 ºC and lasted for 10 min under H_2 atmosphere. In the XRD pattern (Fig. 2b), the peaks at different angle were indexed to diffraction lines from the (100), (002), (101), (102), (110), (103), (112) and (201) planes of La_2O_3 (PDF, 34-0392). Interestingly, the diffraction peaks of La_2O_3 were very strong at plane (101). It might be caused by the well-crystallized large catalyst particles existing in the samples. The above-mentioned results displayed that, unlike the traditional metallic or carbide catalysts, it was the La_2O_3 that acted as a catalyst during the growth of nanotubes. No metal La was formed on the substrate under the hydrogen atmosphere according to Fig. 2b. It was possibly caused by the low standard electrode potential of La_2O_3 ($La^{3+} \rightarrow La$, -2.52 V) which showed that hydrogen could not reduce La_2O_3 to metal La.

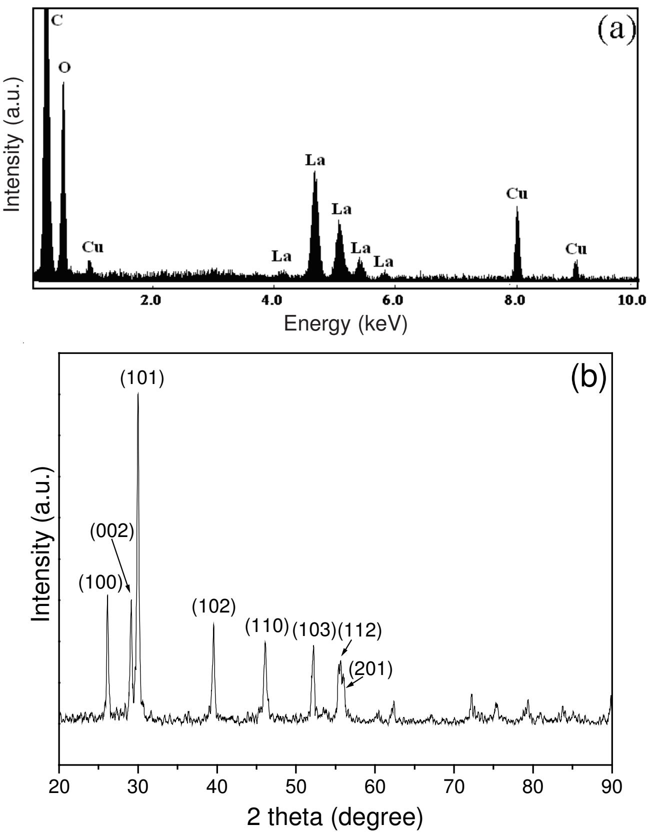

Fig. 2. (a) EDX ananlysis of an individual carbon nanotube with nanoparticle at its end; the Cu signal results from the TEM grid. (b) XRD pattern of the decomposition product of catalyst precursor

It is known that the conventional catalysts such as Fe, Co, Ni and noble metals, such as Au, Pt and Ag, mediate CNT growth *via* their nanoparticles in the liquid phase or highly mobile solid phase with the bulk diffusion of carbon[10-12]. The catalyst particles must be restrained to avoid nanoparticles aggregation and fusion, which significantly reduce the catalytic activity of the nanoparticles. In order to understand the mechanism of CNT nucleation and growth from metallic oxide on a flat surface, we dip the substrate into ethanol solution of $La(NO_3)_3$ and annealing at 900 ºC for 5 min under H_2 atmosphere. Fig. 3a gave the AFM images of the La_2O_3 nanoparticles dispersed on the substrate. Fig. 3b shows the diameter distribution of La_2O_3 nanoparticles gained from AFM measurements. Gaussian fit was done and given the mean diameter of 2.90 nm. It was obvious that most of the particles size of La_2O_3 on the substrate was between 1-5 nm. This observation for SWNT growth provided the experimental evidence that nanosized La_2O_3 particles produced from the ethanolic solution of $La(NO_3)_3$ exhibited catalytic activity for SWNTs growth. Meantime, the result implied that the efficient catalyst depended on the size of nanopaticles more than on the catalysts themselves. The nanotube's outer diameter was directly correlated to the catalyst particle size[27]. It is well-known that Fe-family elements have the catalytic function of graphite formation. A basic understanding of the SWNTs growth from Fe-family is so-called vapour-liquid-solid (VLS) mechanism, in which carbon sources are catalytically decomposed on the nanosized catalyst surface and then coalesce into the metal nanoparticles. Carbon atoms would precipitate from the catalyst to start to grow nanotubes once supersaturation formed. This mechanism was based on the solubility of carbon in metal catalyst. Fe-family metals have high carbon solubility in the bulk phase and strong interaction between them. They can form carbides such as iron carbide, cobalt carbide *etc*. The diffusion of carbon in La_2O_3 was negligibly small compared with that in metal such as Fe and did not catalytically decompose EtOH at low temperature, therefore it is unlikely that bulk diffusion of carbon contributes to SWNT growth. Whereas in the present CVD condition, the facile fluctuation of the nanosized liquid-like structure of the melting La_2O_3 activated EtOH and initiated the nucleation and growth of nanotubes. Actually, lanthanide oxides have catalytic ability for many reactions such as oxidative couple, H/D exchange, decomposition of alcohols, chemical adsorption of NH_3 or CO_2 *etc*.[28]. On the other hand, It is demostrated that defects in a solid could dramatically influence its chemical activity. High temperature treatment on La_2O_3 causes more oxygen vacancies and promotes its catalytic activity[29]. The melting point of La_2O_3 is 2217 ºC, however, it is expected that the melting point of nanosized oxides (< 3 nm) is lower than the growth temperature (700-950 ºC). Thus, high activity for La_2O_3 nanoparticles to catalytically grow SWNTs can be understandable.

We also investigated the effect of the growth temperature on the quality of SWNTs by changing different temperature from the range of 700-950 ºC at 50 ºC increments. We synthesized a series of SWNTs at the different condition respectively and Raman spectroscopy (Fig. 4a) was carried out. As reported in previous publications[30-33], the Raman spectral region

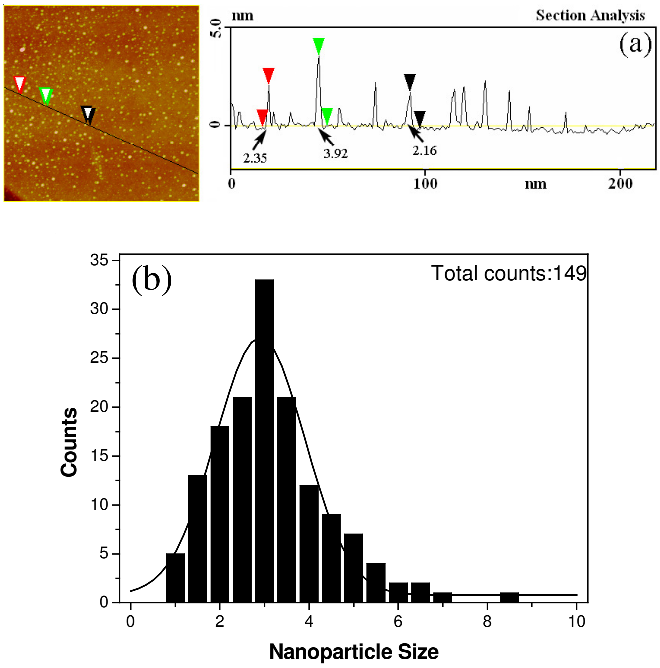

Fig. 3. (a) AFM images and the height measurements of the La_2O_3 nanoparticles on substrate after thermal treatment at 900 ºC for 5 min under H_2 atmosphere. (b) Diameter distribution of La_2O_3 nanoparticles gained from AFM measurements, Gaussian fit is done and given the mean diameter of 2.90 nm

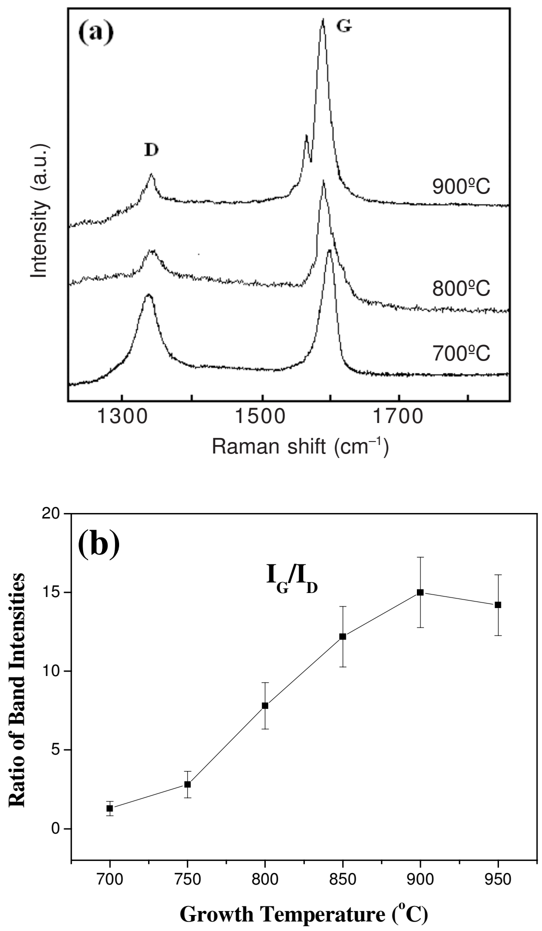

Fig. 4. (a) Representative Raman spectra of the carbon nanotubes synthesized with La_2O_3-EtOH at three different temperatures, (b) the G/D band intensity ratio *versus* reaction temperature

around 1350 cm^{-1} (D band) and 1595 cm^{-1} (G band) were ascribed to disordered carbon and structural defects of the nanotubes and graphitic structure respectively. The peak intensity ratio of the G band to the D-band (G/D value) strongly reflected the purity and quality of SWNTs. Fig. 4a showed the typicial Raman spectra with the vibrational modes (D band and G band) of the carbon nanostructures synthesized at 700, 800 and 900 ºC. A weak peak at 1320 cm^{-1} of the D-band in Fig. 4a indicated that these tubes had good quality at 800 and 900 ºC, however, a strong peak at 700 ºC implied the bad quality of SWNTs. Fig. 4b showed the G/D value of as- grown SWNTs at different temperature. The SWNTs grown at 900 ºC were determined to have the highest G/D ratio, indicating that the optimum crystalline tubal material was obtained. Furthermore, the optimal synthesized temperature region of high-quality SWNT arrays was 850-950 ºC. While those grown at 700 ºC showed the lowest G/D ratio with bad-quality. High temperature should result in better crystallinity of SWNTs and a higher ratio of G to D peaks. More detailed studies of the relationship of tube diameter with growth temperature and helicity were under going in our laboratory.

Conclusion

In summary, we found that La_2O_3 could be a good catalyst for chemical vapour deposition growth of SWNTs. By employing EtOH as carbon source, horizontally superlong SWNT arrays could be generated. Both the growth temperature and nanosized catalysts played important roles in the synthesis of SWNTs with high quality and purity. This result further provided the experimental evidence that the effective catalyst for SWNT growth was more size-dependent than catalysts. The new growth mechanism of nanotubes had been discussed in detail. Further research was needed along controlling the diameter and chirality of SWNTs.

ACKNOWLEDGEMENTS

The work was supported in part by grants from NSFC(21004009) and the Research Program of Jiangxi Province Department of Education (No. GJJ11487).

REFERENCES

1. S. Iijima, *Nature*, **354**, 56 (1991).
2. S. Iijima and T. Ichihashi, *Nature*, **363**, 603 (1993).
3. S.J. Tans, M.H. Devoret, H. Dai, A. Thess, R.E. Smalley, L.J. Geerllgs and C. Dekker, *Nature*, **386**, 474 (1997).
4. A.C. Dillon, K.M. Jones, T.A. Bekkedahl, C.H. Kiang, D.S. Bethune and M.J. Heben, *Nature*, **386**, 377 (1997).
5. S.J. Tans, A.R.M. Verschueren and C. Dekker, *Nature*, **393**, 49 (1998).
6. A.G. Rinzler, J.H. Hafner, P. Nikolaev, P. Nordlander, D.T. Colbert, R.E. Smalley, L. Lou, S.G. Kim and D. Tománek, *Science*, **269**, 1550 (1995).
7. J. Lu, S.S. Yi, T. Kopley, C. Qian, J. Liu and E. Gulari, *J. Phys. Chem. B*, **110**, 6655 (2006).
8. W.Q. Deng, X. Xu and W.A. Goddard, *Nano Lett.*, **4**, 2331 (2004).
9. L.H. Liang, F.D. Liu, X. Shi, W.M. Liu, X.C. Xie and H.J. Gao, *Phys. Rev. B*, **72**, 35453 (2005).
10. D. Takagi, Y. Homma, H. Hibino, S. Suzuki and Y. Kobayashi, *Nano Lett.*, **6**, 2642 (2006).
11. S. Bhaviripudi, E. Mile, S.A. Steiner and J. Kong, *J. Am. Chem. Soc.*, **129**, 1516 (2007).
12. D. Takagi, Y. Kobayashi, H. Hibino, S. Suzuki and Y. Homma, *Nano Lett.*, **8**, 832 (2008).
13. W. Zhou, Z. Han, J. Wang, Y. Zhang, Z. Jin, X. Sun, Y. Zhang, C. Yan, and Y. Li, *Nano Lett.*, **6**, 2987 (2006).

14. M. Ritschel, A. Lenonhardt, D. Elefant, S. Oswald and B. Büchner, *J. Phys. Chem. C*, **111**, 8414 (2007).
15. Y. Zhang, W. Zhou, L. Ding, Z. Zhang, X. Liang and Y. Li, *Chem. Mater.*, **20**, 7521 (2008).
16. Y. Qian, C.Y. Wang and B. Huang, *Nanoscale Res. Lett*., **5**, 442 (2010).
17. H. Yoshida, S. Takeda, T. Uchiyama, H. Kohno and Y. Homma, *Nano Lett*., **8**, 2082 (2008).
18. D. Yuan, L. Ding, H. Chu, Y. Feng, T.P. McNicholas and J. Liu, *Nano Lett.*, **8**, 2576 (2008).
19. B. Liu, W. Ren, L. Gao, S. Li, Q. Liu and H.M. Cheng, *J. Phys. Chem. C*, **112**, 19231 (2008).
20. B. Liu, W. Ren, L. Gao, S. Li, S. Pei, C. Liu, C. Jiang and H.M. Cheng, *J. Am. Chem. Soc.*, **131**, 2082 (2009).
21. S.A. Steiner III, T.F. Baumann, B.C. Bayer, R. Blume, M.A. Worsley, W.J. MoberlyChan *et al.*, *J. Am. Chem. Soc.*, **131**, 12144 (2009).
22. C. Kocabas, S.H. Hur, A. Gaur, M.A. Meitl, M. Shim and J.A. Roger, *Small*, **1**, 1110 (2005).
23. S.M. Huang, M. Woodson, R. Smalley and J. Liu, *Nano Lett*., **4**, 1025 (2004).
24. S. Han, X. Liu and C. Zhou, *J. Am. Chem. Soc*., **127**, 5294 (2005).
25. A. Jorio, R. Saito, J.H. Hafner and C.M. Lieber, *Phys. Rev. Lett.*, **86**, 1118 (2001).
26. A. Jorio, C. Fantini and M.A. Pimenta, *Phys. Rev. B*, **71**, 075401 (2005).
27. S.B. Andrews, Sinnott, R. Andrews, D. Qian, A.M. Rao and Z. Mao, *Chem. Phys. Lett.*, **315**, 25 (1999).
28. G. Adachi, N. Imanaka and Z.C. Kang, Binary Rare Earth Oxides, Kluwer Academic Publishers (2004).
29. G.R. Haire and L. Eyring, Handbook on the Physics and Chemistry of Rare Earth, North-Holland, Amsterdam, vol. 18, p. 413 (1994).
30. Y. Qian, S.M. Huang, F.L. Gao, Q.R. Cai and L.J. Zhang, *J. Phys. Chem. C*, **113**, 6983 (2009).
31. S.M. Huang, Y. Qian, J.Y. Cheng, Q.R. Cai, L. Wang, S. Wang and W.B. Hu, *J. Am. Chem. Soc*., **130**, 11860 (2008).
32. Y. Qian, S.M. Ji, S.M. Huang and W.B. Hu, *Mater. Lett.*, **63**, 1393 (2009).
33. Y. Qian, B.Huang, F.L. Gao, C.Y. Wang and G.Y. Ren, *Nanoscale Res. Lett.*, **5**, 1578 (2010).